Line shape and mechanisms of nonlinear cyclotron resonance in bismuth

G. I. Leviev and M. R. Trunin

Institute of Solid State Physics, USSR Academy of Sciences
(Submitted 11 July 1984)
Zh. Eksp. Teor. Fiz. **90**, 674–685 (February 1986)

Nonlinear cyclotron resonance in bismuth is investigated experimentally at various microwave-field polarizations. The cases of an alternating field parallel and perpendicular to the metal surface are considered. It is shown that the resonance line shape is determined by interference of two nonlinearity mechanisms, one connected with the magnetic field of the wave, and the other with the electric field perpendicular to the metal surface. The resonance fields for the electrons of the central section and of the limiting point agree well with those calculated from the McClure and Choi model of the Fermi surface. Results of a numerical calculation of the nonlinear-cyclotron-resonance waveform are presented and lead to inversion of the resonances with increasing incident-wave amplitude, in agreement with experiment.

INTRODUCTION

A metallic sample irradiated by a sufficiently strong electromagnetic wave of frequency ω, has nonlinear properties. At low frequencies, when $\omega/v \ll 1$ (v is the frequency of the collisions between the electron and the scatterers) the main source of the nonlinearity is the magnetic field of the wave.[1] This field can be regarded as quasistatic with respect to the electron motion, but as spatially inhomogeneous. At microwave frequencies, $\omega/v \gg 1$, both spatial and temporal dispersion of the nonlinear characteristics of a metal are important. Kopasov[2–4] investigated the nonlinear response of a metal under cyclotron-resonance conditions, in the limit of weak nonlinearity due to an alternating magnetic field. He has shown that at a frequency 2ω double that of the incident wave the coefficient of nonlinear reflection increases significantly if the following conditions are met:

$$\omega = n\Omega, \tag{1}$$
$$\omega = (n-\tfrac{1}{2})\Omega, \quad n = 1, 2, 3 \ldots \tag{2}$$

($\Omega = eH/mc$ is the cyclotron frequency).

We shall refer to cyclotron resonances defined by relation (1) as integer resonances. The presence of half-integer resonances (2) distinguishes the resonance conditions (1) and (2) from the condition of linear cyclotron resonance.

In an experimental investigation of nonlinear reflection of an electromagnetic wave at frequency 2ω in Bi in the region of electron[5] and hole[6] cyclotron resonances, Gantmakher and the present authors have actually observed a steep growth of the signal in magnetic fields satisfying the condition (1). In half-integer resonances, the generation was observed to decrease rather than increase. Édel'man[7] has pointed out that a correlation exists in the magnetic-field dependences of the squared product of the sample over the magnetic field and the nonlinear-reflection coefficient.

The reason for the different forms of the integer and half-integer resonances in the experiments of Refs. 5 and 6 was not clearly explained. It was assumed that the resonant changes of the linear conductivity of the metal at double the frequency must be taken into account in the interpretation of the experiments. It is known, however, that these changes do not exceed several percent, whereas the nonlinear-reflection coefficient in integer resonances increases by two decades. It was also noted[4] that besides the nonlinearity due to the magnetic field of the wave an important role can be assumed in the experiment of Ref. 5 by some additional nonlinearity, that alters the form of the resonance and is due to the presence of a large electric-field component of frequency ω and perpendicular to the sample surface. At normal incidence of the wave on the sample,[2–4] the resonances (1) and (2) had the form of emission maxima independently of the conditions under which the electrons were reflected from the surface.

We show in the present paper that at any polarization of the exciting microwave field the different forms of resonances (1) and (2) are due to interference of two nonlinearity mechanisms. The first stems from the wave's magnetic field, and the second is due to the anisotropy, in Bi, of the electric field perpendicular to the sample surface. In the presence of both fields, the resonances (1) and (2) can take the form of either peaks or dips of radiation. If one manages to leave only one field in the metal, the dependence of the nonlinear reflection coefficient on the external magnetic field takes the theoretically predicted form—all the resonances appear as maxima.

The forms of the resonances (1) and (2) depend also on the amplitude of the incident wave. When it increases, the nonlinear signal first grows in proportion to the square of the incident-wave amplitude, and then much more slowly. The deviation from the quadratic regime sets in first in integer resonances and leads, in the upshot, to their inversion—the emission at resonance becomes weaker than in a nonresonant field. We shall discuss a model that takes into account the possible nonlinearity mechanisms and permits a numerical calculation of the evolution of the forms of cyclotron resonances (1) and (2).

PROCEDURE

We studied in the experiment the nonlinear microwave response produced in Bi at a frequency 2ω on irradiation of the sample by an electromagnetic wave of frequency $\omega/2\pi = 9.3$ GHz. The main difference between the experi-
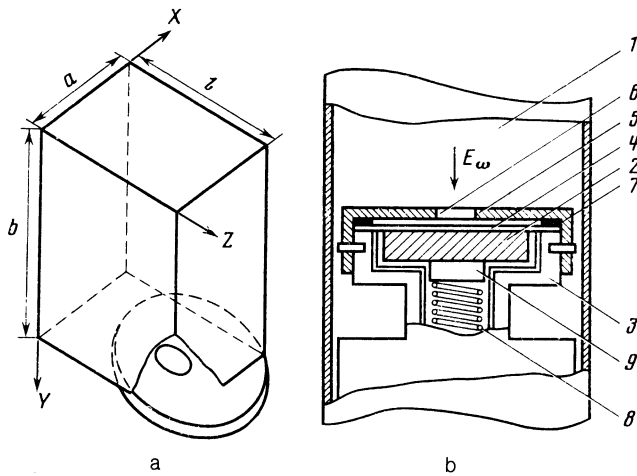
FIG. 1. Bimodal rectangular (a) and cylindrical (b) cavities. The metallic parts of the structure are shown shaded in Fig. b.

ments described below and those of Refs. 5 and 6 is in the method used to irradiate the sample.

In the investigation of second-harmonic generation in a microwave field parallel to the surface, the sample was clamped to a diaphragm on the bottom of a bimodal rectangular cavity (Fig. 1a). The cavity operated on the H_{011} mode at the frequency ω and the H_{022} mode at double this frequency. The electric and magnetic fields of both modes were parallel. The electric field of the H_{011} mode had a single nonzero component E_x. The force lines of this field formed a bundle of straight lines parallel to the x axis, with maximum density at $y = b/2$ and $z = l/2$. The magnetic force lines were closed concentric rings that encircled this bundle.

The bottom of the cavity is a metallic foil 0.1 mm thick. The diaphragm is a round aperture with center ($x = a/2$, $z = l/e$) placed in the antinode of the magnetic field H_z of the H_{022} mode. Hereafter, the amplitude of the alternating magnetic field on the surface of a sample in a rectangular cavity is taken to mean

$$H_\sim = 4\left[\frac{\pi l P_\bullet Q}{\omega b a (l^2 + b^2)}\right]^{1/2}, \qquad (3)$$

and is equal to the amplitude of the field H_z of frequency ω at the center of the sample. P_ω, Q, and ω in Eq. (3) are the dissipated power, the unloaded Q, and the cavity frequency.

Besides experiments with linearly polarized transverse fluxes of the incident and excited waves, we investigated harmonic generation in an electric microwave field perpendicular to the sample surface. We used for this purpose cylindrical cavity 1, tuned to the frequencies ω and 2ω (Fig. 1b). At the frequency 2ω the cavity operated in the H_{111} mode. At the frequency ω we excited in the cavity an E_{010} mode whose electric force lines were parallel to the cavity axis and increased in density as this axis was approached. The magnetic field of the E_{010} mode is zero on the cavity axis and reaches a maximum $H_\sim$ at a distance 9 mm from the axis of the cavity used by us.

Sample 2 was mounted on a contactless teflon piston 3.

A metallic cover 5, with a round opening (diaphragm 6) was placed on top of the piston through a thin teflon film.[4] The inside periphery of the cover was coated with a layer of absorber 7. The sample was clamped to the diaphragm with a spring 8 that pressed against a gasket 9 made of cloth-reinforced laminate. The diaphragm diameter was varied in the experiment from 17.6 to 3 mm, which made it possible to obtain in the sample various ratios of the amplitudes of the magnetic field and of the electric field perpendicular to the sample surface.

The experiments were performed at various incident-wave power levels, and the alternating magnetic field strength could be varied in the range from 0.1 to 10 Oe. In the interval 1 Oe $< H_\sim < 10$ Oe the cavities were excited by a magnetron pulses with a repetition frequency 40 Hz and duration 2 μs. At very low signal levels, $H_\sim < 1$ Oe, the sample was irradiated with a microwave generator modulated by rectangular pulses at a frequency 5 kHz. The double-frequency radiation was picked up with a heterodyne receiver whose output signal was fed either to an integrator or to a narrow-band amplifier with a lock-in detector and from the latter to the Y input of an automatic plotter, whose X input was the sweep of the external magnetic field. The magnetic field was produced with a Helmholtz system compensated for the earth's field. The magnetic field could be rotated through any angle in the plane of the sample, accurate to 20'.

The experiments were performed on several Bi samples with $n\|C_3$, in the form of disks 17.8 mm in diameter. The deviation of the C_3 axis from normal did not exceed 1.5°. The cavity construction provided for the possibility of rotating the sample through an arbitrary angle in the experiment with liquid helium. All the experimental plots in this paper were obtained at $T = 1.5$ K.

EXPERIMENT

We measured in the experiment the power $P_{2\omega}$ of the wave of frequency 2ω reflected from the sample, as a function of the external magnetic field H. Figure 2 shows a typical plot of the $P_{2\omega}$ (H) signal at different polarizations of the microwave field, which was parallel to the sample surface. In a geometry $H_\omega\|H_{2\omega}\perp C_2$, $H\|C_2$ and with exact tuning, the signal amplitude decreases drastically and is not observed below $H_\sim = 10$ Oe. At an insignificant deviation from exact tuning (lower curve of Fig. 2) the resonance curve has a simple form: the integer (1) and half-integer (2) resonances are manifested as emission maxima, with the signal amplitude larger in the integer than in the half-integer resonances. The small maximum on the right of the first resonance is due to cyclotron resonance of the electrons from the vicinity of the limiting point. With further increase of the angle between H and H_ω, the signal $P_{2\omega}$ (H) increase still further, but the form of the resonance lines changes significantly, and at $H\|H_\omega\|H_{2\omega}\|C_2$ (upper curve of Fig. 2) the half-integer resonances take the form of minima.

Figure 3 shows the experimental plots of $P_{2\omega}$ (H) in the $H_\omega\|H_{2\omega}\perp C_1$, geometry and with angle 0.5° between H and C_1, for different amplitudes $H_\sim$ of the electromagnetic wave incident on the sample. The solid lines in the inset[1] show the
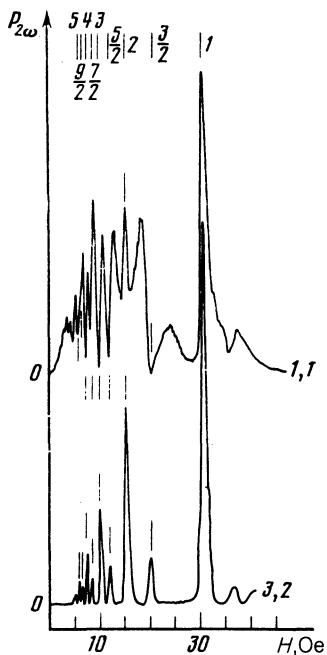
FIG. 2. Typical plot of $P_{2\omega}(H)$ signal of Bi sample with $n\|C_3$. $\mathbf{H}\|\mathbf{H}_\omega\|\mathbf{H}_{2\omega}\|C_2$ for the upper curve, $\mathbf{H}_\omega\|\mathbf{H}_{2\omega}\perp C_2$ for the lower, and the angle between $\mathbf{H}$ and C_2 is $0.5°$. The zero levels $P_{2\omega}=0$ and the amplitude $H_\sim$ in oersteds (the numbers on the right) are indicated for each curve. The vertical strokes mark the positions of the (1) and (2) resonances as calculated from the known cyclotron masses.[8]

FIG. 4. Radiated power $P_{2\omega}$ vs the power P_ω incident on the sample in integer ($n=3$) and half-integer ($n=5/2$) resonance fields.

cyclotron masses, calculated from the spectrum of McClure and Choi (Ref. 9, first set of parameters), of the electrons of the central section of the β ellipsoid and of the turning point as functions of the angle φ of rotation of the magnetic field $\mathbf{H}$

in the sample plane. The experimental locations of the resonance 1β (circles) and of the maximum on its right (black dots) fit splendidly the calculated plot. No resonance signal from electrons of the limiting-point vicinity are observed in investigations of linear cyclotron resonance in this geometry.

The upper plot of Fig. 3 was obtained at a higher amplitude $H_\sim$ of the high-frequency field in the cavity. It can be seen that the ratio of the radiation intensities in the integer and half-integer resonances has changed: the half-integer resonances increase more rapidly with increasing $H_\sim$. The
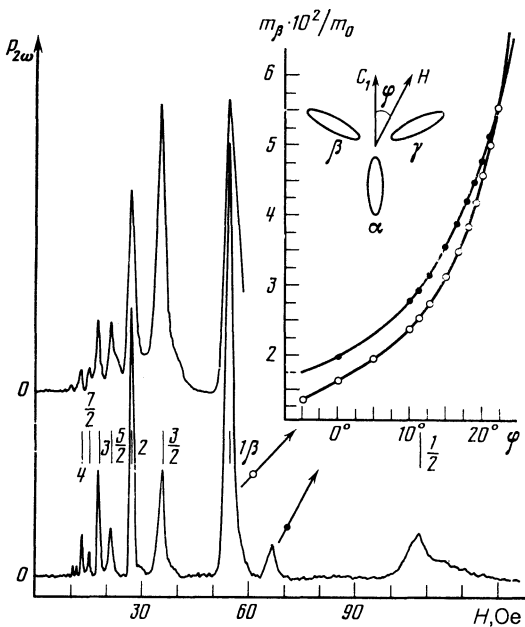

FIG. 3. Plots of $P_{2\omega}(H)$ for $\mathbf{H}_\omega\|\mathbf{H}_{2\omega}\perp C_1$ with angle $0.5°$ between $\mathbf{H}$ and C_1. The $H_\sim$ amplitudes for the lower and upper curves are 0.6 and 5.1 Oe, respectively. The zero levels $P_{2\omega}=0$ are indicated. The curves are plotted at different sensitivities.
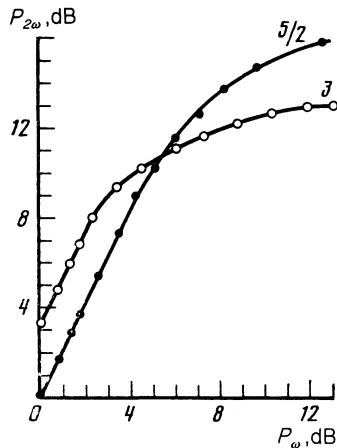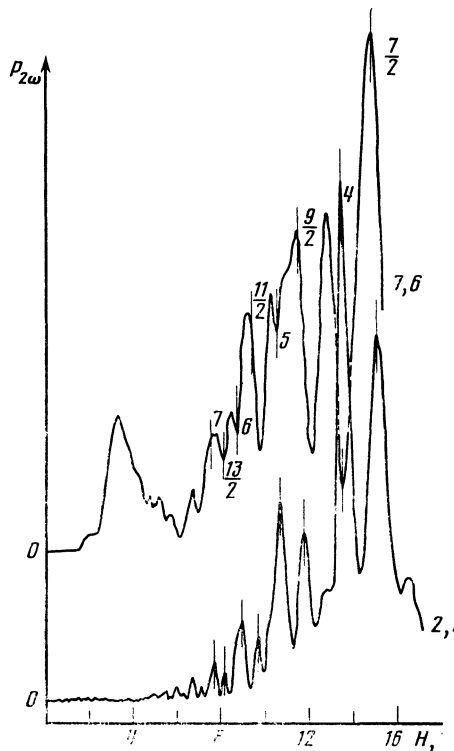

FIG. 5. Inversion of cyclotron-resonance lines with increasing $H_\sim$; the values of $H_\sim$ (in oersteds) are indicated on the right of the curves. The curve are plotted with different sensitivities; $\mathbf{H}_\omega\|\mathbf{H}_{2\omega}\perp C_1$, $\triangleleft\mathbf{H}$, $C_1=0.5°$.
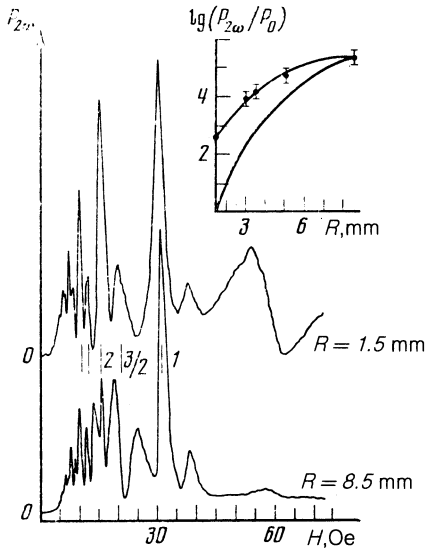
FIG. 6. Plots of $P_{2\omega}$ (H) for Bi sample placed in the cylindrical cavity; $\mathbf{n}\|C_3,\mathbf{H}\|C_2$. To the right of the curves are indicated the values of the radius R of the diaphragm on the sample surface.

reason for this change is that integer resonances deviate from the quadratic relation

$$P_{2\alpha} \sim P_\omega{}^2 \qquad (4)$$

earlier than the half-integer ones (Fig. 4). The saturation of the resonance signal is accompanied by broadening of the resonance line. The saturation results in inversion of the cyclotron resonance lines (Fig. 5). Inversion sets in earlier the weaker the field H that is at resonance.

Figure 6 shows plots of $P_{2\omega}$ (H) at $\mathbf{H}\|C_2$ for a sample in a microwave whose electric field is perpendicular to the sample surface. The plots were obtained at different diaphragm radii R. The alternating magnetic field H_ω on the sample decreases with decreasing R. Knowing the direction of the linear current $\mathbf{j}^{(2\omega)}$ (r,H) (vide infra) and the vector eigenfunction $\mathbf{E}^{(2\omega)}$ (r,H) normalized in the cavity volume V and corresponding to the mode at the doubled frequency, we can numerically calculate the relative power contribution

$$P_{2\omega}(H) \sim \left[\int_V \mathbf{j}^{(2\omega)}(r,H)\mathbf{E}^{(2\omega)}(r,H)dV \right]^2 , \qquad (5)$$

made to the measured power $P_{2\omega}$ (R) and due only to the nonlinearity caused by the magnetic field H_ω of the wave. This dependence corresponds to the lower curve of the inset of Fig. 6. The experimental points measured in a field $H = 31.5$ Oe show a much slower decrease of the radiation. This indicates directly that at small diaphragm radii the entire process of harmonic generation in the sample is due to the external perpendicular electric field.

NONLINEAR CURRENT AND NONLINEARITY MECHANISMS

An electromagnetic wave of frequency ω incident on the surface of a Bi sample penetrates into the sample (y axis) and produces in it a nonlinear current $j^{(2\omega)}$ (y) at the doubled frequency 2ω:

$$j_\alpha^{(2\omega)} (y) = \int\int \sigma_{\alpha\beta\gamma}^{(2\omega)} (y,y',y'')E_\beta^{(\omega)} (y')E_\gamma^{(\omega)} (y'')dy' \, dy'',$$

$$j^{(2\omega)} (y,t) = j^{(2\omega)} (y)e^{-2i\omega t} + \text{c.c.} \qquad (6)$$

Here $\sigma_{\alpha\beta\gamma}^{(2\omega)}$ is the nonlinear conductivity tensor and $E^{(\omega)}$ is the alternating electric field with fundamental frequency ω. The nonlinear current plays the role of a source that excites oscillations of the harmonic in the cavity and enters in the Maxwell equations for the fields of the harmonic as a given extraneous current.

The quantity recorded in experiment is $P_{2\omega}$ (H) defined by relation (5). The function $E^{(2\omega)}$ (r,H) describes in the linear approximation the field distribution at the doubled frequency inside the metal. This function is used to express the linear impedance ζ of the metal: $\zeta(H) \propto [E_{2\omega}{}'(0,H)]^{-1}$. To find the form of the function $P_{2\omega}$ (H) we must calculate the current $j^{(2\omega)}$ (H).

The nonlinear-conductivity tensor and the current (6) are calculated from the kinetic equation in which the nonlinear terms are retained. It was assumed in Refs. 2–5 that the main contribution to the nonlinearity is made by the Lorentz force due to magnetic field of the wave. Strictly speaking, however, for the semimetal Bi it is necessary to take into account also the nonlinearity quadratic in the electric field.

In second order in the field, the general connection between the current and the fields can be schematically represented in the form

$$j^{(2\omega)} = \hat{\beta}E^{(\omega)}E^{(\omega)} + \hat{\alpha}E^{(\omega)}H^{(\omega)}. \qquad (7)$$

In the general case the third-rank tensors $\hat{\beta}$ and $\hat{\alpha}$ depend on the frequency, on the wave vector $\mathbf{k}$, and on the external magnetic field $\mathbf{H}$. Note that in a medium with inversion center (such as Bi) the tensor $\hat{\beta}$ vanishes as $k\rightarrow 0$, while the pseudotensor $\hat{\alpha}$ remains finite. At low frequencies the nonlinearity is therefore due entirely to the magnetic Lorentz force. In the microwave band, when account is taken of spatial dispersion, the tensor $\hat{\beta}$ is not equal to zero. The exact ratio of the first and second terms in the expansion (7) can be obtained only by a microscopic analysis, but here we confine ourselves to a comparison of the forces $F_E = eE^{(\omega)}$ and $F_H = ev_FH^{(\omega)}/c$ responsible for the nonlinearity.

If the fields $E^{(\omega)}$ and $H^{(\omega)}$ are Maxwellian, we have on the sample surface

$$E^{(\omega)} = (\omega/ck)H^{(\omega)}, \qquad F_E/F_H = \omega/v_Fk \sim \omega\delta/v_F, \qquad (8)$$

where δ is the skin-layer depth and v_F is the Fermi velocity. It follows from (8) that in typical metals at $\omega \sim 10^{10}$ s^{-1} we have the ratio $\delta/v_F \sim 10^{-13}$ s and $F_E \ll F_H$. In Bi at $\omega \approx 6 \cdot 10^{10}$ s^{-1} we have in a zero magnetic field $\delta \approx 10^{-4}$ cm (Ref. 10). Using for the Bi electrons the value $v_F \approx 6 \cdot 10^7$ cm/s, we get from (8) $F_E = 0.1\, F_H$. In a nonzero external magnetic field the ratio F_E/F_H increases additionally, because excitation of cyclotron waves in Bi increases the penetration depth of the alternating field.[7,11] For Bi it is therefore necessary to take into account both the magnetic and the electric nonlinearities, i.e., both terms of the expansion (7).

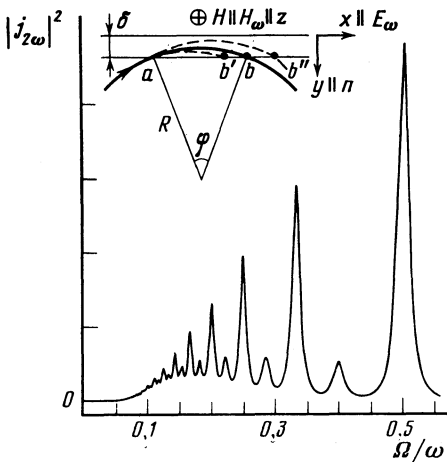Let us examine in greater detail the forces acting on an electron in the skin layer, and the mechanism whereby the

G. I. Leviev and M. R. Trunin   395

FIG. 7. The dependence, calculated from (21), of the squared modulus of the nonlinear current on the external magnetic field **H**; $\omega/\nu = 20$. The inset shows schematically the electron trajectory in the skin layer.

current at the doubled frequency 2ω is produced. In agreement with experiment, we assume that the following conditions are met:

$$\tau_0 \sim (\delta/\Omega v_F)^{1/2} = (\delta mc/v_F H)^{1/2} \ll 2\pi/\omega, \qquad \delta \ll R. \qquad (9)$$

Here τ_0 is the time required by an electron moving in a field **H**$\|z$ along a circular orbit of radius R to pass through the skin layer. The electron revolution time is $T_0 = \tau_0 + \tau_d$, where τ_d is the time of motion in the interior of the metal beyond the skin-layer boundary. In the linear theory it is assumed that the alternating field does not perturb the electron trajectory (section ab on the inset of Fig. 7). At larger electromagnetic-wave amplitudes the influence of the alternating field must be taken into account. Depending on the phase of this field, an electron entering the skin layer at a point a leaves the layer at a point b' or b''. This distortion of the electron trajectory is due to the action of the alternating force F_y:

$$F_y = eE_y e^{-i\omega t} + (e/c) v_F H_z e^{-i\omega t} + \text{c.c.} \qquad (10)$$

At normal incidence of the electromagnetic wave on the sample surface, the electric and magnetic field components $E_y^{(\omega)}$ and $H_z^{(\omega)}$ appear in the skin layer because of the anisotropy of the Fermi surface of Bi. To simplify the equations that follow, we have assumed in (10) that $E_y^{(\omega)}$ and $H_z^{(\omega)}$ are in phase. The resultant action of either field on the electron is the same — the onset of a force (10) that changes the time $\tau(t)$ of passage of the electron through the skin layer. As a result, if the alternating Lorentz force (10) is weaker than the dc field

$$\frac{H_z + cE_y/v_F}{H} = \xi < 1, \qquad (11)$$

we can write for the time of passage $\tau(t)$

$$\tau(t) = \tau_0(1 - \xi \cos \omega t). \qquad (12)$$

The nonlinearity in our problem is thus due to the change of the time of the electron interaction with the alter-

nating electric and the magnetic fields in the skin layer. We calculate now within the framework of this model the nonlinear current $j^{(2\omega)}$ in the cyclotron-resonance region:

$$j^{(2\omega)} = en_0 (\delta/R)^{1/2} V^{(2\omega)}, \qquad (13)$$

where $n_0(\delta/R)^{1/2}$ is the number of effective electrons and $V^{(2\omega)}$ the velocity of the electrons.

Assume that the electron left the skin layer at the instant t. According to (9), the phases of the alternating fields change little during the time of passage through the skin layer. Therefore in the preceding revolution the electron emerged from the skin layer at the instant

$$t_1 = t - \tau(t_1) - \tau_d = t - T_0 + \xi\tau_0 \cos \omega t. \qquad (14)$$

Similarly, for the two, three, and n earlier revolutions the emergence time was $t_2, t_3, \dots, t_n$:

$$t_2 = t - \tau(t_1) - \tau_d$$
$$= t - 2T_0 + \xi\tau_0\{\cos \omega t + \cos[\omega(t - T_0 + \xi\tau_0 \cos \omega t)]\},$$
$$t_3 = t_2 - \tau(t_2) - \tau_d = t_2 - T_0 + \xi\tau_0 \cos \omega t_1, \qquad (15)$$
$$t_n = t_{n-1} - T_0 + \xi\tau_0 \cos \omega t_{n-1}.$$

During the time $\Delta t \sim \tau_0$ of each stay of the electron in the skin layer it interacts with the tangential electric field $E^{(\omega)}$. The electron velocity is therefore always increased in the same direction, parallel to the metal surface; for example, in the nth passage through the skin layer

$$\Delta v_n \approx (e\tau_0/m)E_x \exp(-i\omega t_n) + \text{c.c.} \qquad (16)$$

The total velocity increment is obtained by summing Δv_n from (16) over all the times of stay in the skin layer, with a weight $\exp(-n\nu T_0)$ (ν is the collision frequency) that takes into account the exponential damping of the contribution from each passage

$$\Delta V = \frac{eE_x}{m} \tau_0 e^{-i\omega t} \sum_{n=1}^{\infty} \left\{ e^{-n\nu T_0} e^{in\omega T_0} \right.$$
$$\left. \times \exp\left[-i\omega\xi\tau_0 \sum_{k=0}^{n-1} e^{-i\omega t_k} \right] \right\} + \text{c.c.}, \qquad (17)$$

$$t_k = t_{k-1} - T_0 + \xi\tau_0 \cos \omega t_{k-1}, \qquad t_0 = t.$$

For the term in the square brackets in (17) we can write

$$-i\omega\xi\tau_0 \sum_{k=0}^{n-1} e^{-i\omega t_k}$$

$$= -i\omega\xi\tau_0 e^{-i\omega t} \left[1 + \sum_{m=1}^{n-1} e^{i\omega m T_0} \exp\left(-i\omega\xi\tau_0 \sum_{l=0}^{m-1} e^{-i\omega t_l} \right) \right]. \qquad (18)$$

We are interested in the increment of the velocity $V^{(2\omega)} \propto e^{-2i\omega t}$ at the doubled frequency. An analytic expression for $V^{(2\omega)}$ is obtained from (17) by expanding the exponential in powers of the small exponent (18). Let us ascertain the limits imposed on the parameter ξ in such an expansion. We note for this purpose that the maximum value of the sum over l in (18) is equal to m, and if the inequality (11) holds the expression in the square brackets of (18) is a

finite geometric progression with exponent $\exp(i\omega T_0)$. It can be easily seen that at $\omega = n\Omega + \gamma(\gamma \ll \Omega)$, i.e., near integer resonances, the sum of the terms of this progression is equal to n, while far from integer resonances, meaning also for half-integer ones, the sum is of the order of 1. This means that in integer resonances the current $j^{(2\omega)}$ ceases to be a quadratic function of the incident-wave field sooner than in half-integer ones. Since the significant terms in (17) are those with $n \lesssim \Omega/\nu$, the condition that (18) be small takes for integer resonances the form

$$\xi \ll \frac{\nu}{\omega}\left(\frac{R}{\delta}\right)^{1/2} . \qquad (19)$$

In half-integer resonances the quadratic regime extends to alternating-field amplitudes that are Ω/ν times stronger:

$$\xi \ll \frac{\Omega}{\omega}\left(\frac{R}{\delta}\right)^{1/2} . \qquad (20)$$

If the inequalities (11), (19), and (20) hold, we obtain from (17), accurate to a numerical coefficient of order unity, an expression for the nonlinear current (13):

$$j^{(2\omega)} = \frac{e^2\omega n_0}{m\Omega^2}\left(\frac{\delta}{R}\right)^{1/2}\left(H_z + \frac{c}{v_F}E_y\right)\frac{E_x}{H}e^{-2i\omega t}e^{(i\omega - \nu)T_0}[1$$
$$-e^{(i\omega - \nu)T_0}]^{-1}[1 - e^{(i2\omega - \nu)T_0}]^{-1}. \qquad (21)$$

The denominator of (21) contains resonant factors for both integer (1) and half-integer (2) resonances. Furthermore, inasmuch as for integer resonances both square brackets reach simultaneously a minimum value ν/Ω, the singularities in these resonances will be stronger than in half-integer ones.

DISCUSSION. COMPARISON WITH EXPERIMENT

The reflected power $P_{2\omega}$ (H) determined by (5) increases by more than an order of magnitude at resonance (see, e.g., Fig. 2), whereas the change of the impedance in linear cyclotron resonance does not exceed several percent. We can therefore neglect in (5) the dependence of the linear characteristic of the metal on the field H, and assume that the form of the function $P_{2\omega}$ (H) is determined by the dependence of the nonlinear current squared, $|j^{(2\omega)}$ $(H)|^2$, on the magnetic field.

Figure 7 shows the function $|j^{(2\omega)}$ $(H)|^2$ calculated from (21) at $\omega/\nu = 20$. The resonances (1) and (2) take the form of maxima. The singularities for integer resonances are stronger than for half-integer ones. A similar plot was calculated for $P_{2\omega}$ (H) in Ref. 4, where an ellipsoidal model of the Fermi surface of B was used. We note the satisfactory similarity of the resonance curves calculated in Ref. 4 and shown in Fig. 7 to the experimental lower plots of Figs. 2, 3, and 5.

With increasing amplitude of the electromagnetic wave incident on the sample, the shape of the resonance lines changes (see Figs. 3 and 5). This change is due to violation of conditions (19) and (20) and to deviation from the quadratic regime (4). The first to be violated is condition (19), so that the integer resonances saturate sooner. As a result, the amplitudes of the half-integer resonances becomes larger than those of the integer ones (see Fig. 3). At the same time,
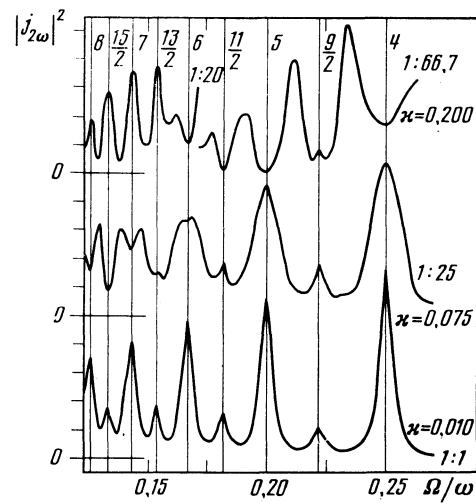

FIG. 8. Numerical calculation of $|j^{(2\omega)}$ $(H)|^2$ at $\omega/\nu = 30$ and at different values of the parameter $\varkappa = \xi\Omega(\delta/v_F\omega)^{1/2}$. The zero levels $|j^{(2\omega)}$ $(H)|^2 = 0$ are marked for each curve. The numbers on the right sides of the curves are the factors by which the amplitude $|j^{(2\omega)}|^2$ has increased compared with the lower curve.

the background signal in the interval between the resonance lines at $H_\sim < 10$ Oe always increases quadratically, so that at a sufficiently high incident power the amplitude of this background already exceeds the amplitude of the resonance signal, leading to inversion of the resonance lines (cf. Fig. 5).

Using the model described in the preceding section, we calculate $|j^{(2\omega)}$ $(H)|^2$ for the case when conditions (19) and (20) are not met. Substituting expression (17) in the form of a Fourier series, we separate the second harmonic of this series. The numerically calculated function $|j^{(2\omega)}$ $(H)|^2$ at different values of the parameter $\varkappa = \xi\Omega[\delta/(v_F\omega)]^{1/2}$ is shown in Fig. 8. The lower curve ($\varkappa = 0.01$, $\xi \ll 1$) corresponds to validity of conditions (19) and (20), and the form of the resonance curve is similar to that shown in Fig. 7. With increasing $\varkappa$, the resonance lines broaden and, starting with weaker fields H, inversion of the resonances takes place. Finally, at the highest alternating-field amplitude (upper curve of Fig. 8), after the integer resonances with numbers $n = 4$ and 5 were inverted, the half-integer resonance $n = 9/2$ still retained the shape of a maximum. We note that $\xi \lesssim 1$ in this case. The described behavior of $|j^{(2\omega)}$ $(H)|^2$ agrees with the experimental $P_{2\omega}$ (H) dependence shown in Figs. 3 and 5.

We proceed now to a discussion of the upper curve of Fig. 2. To interpret this experiment we must take into account two circumstances left out of our analysis—the anisotropy of the carrier dispersion in Bi, and the phase difference between the electric and magnetic forces in (10), a difference that depends on the external magnetic field H. We shall show now that when this difference is taken into account the simple form of the resonance lines on the lower curve of Fig. 2 is obtained by excluding one of the nonlinearity mechanisms previously considered in (7), viz., the nonlinearity quadratic in the alternating electric field. In the presence of both terms in (7) and with account taken of the phase differ-

ence between them, the signal $P_{2\omega}(H)$ should increase, and the form of the resonance line should change substantially, as is indeed observed on going from the lower to the upper curve of Fig. 2.

Let $\mathbf{H} \| C_2 \| z$, $\mathbf{n} \| C_3 \| y$. In this case Bi has a nonzero component of the linear-conductivity tensor σ_{xy} ($\sigma_{xz} = \sigma_{yz} = 0$). It follows from the Maxwell equations that

$$j_y^{(\omega)} = \sigma_{yy} E_y^{(\omega)} + \sigma_{yx} E_x^{(\omega)} = 0, \qquad E_y^{(\omega)} = -(\sigma_{yx}/\sigma_{yy}) E_x^{(\omega)} \qquad (22)$$

and consequently a normal electric field $E_y^{(\omega)}$ is produced in the sample only if $E_x^{(\omega)} \neq 0$. On the upper plot of Fig. 2 we have $E_x^{(\omega)} \neq 0$, and on the lower $H \| E_z^{(\omega)}, E_x^{(\omega)} = E_y^{(\omega)} = 0$.

The radiation recorded in experiment always has $\mathbf{E}_{2\omega} \| \mathbf{E}_\omega$, and according to (5) the value of $P_{2\omega}$ is determined by the scalar product $\mathbf{j}_{2\omega} \cdot \mathbf{E}_{2\omega}$. It can be shown from symmetry considerations that at $\mathbf{H} \| C_2$ or $\mathbf{H} \| C_1$ the nonlinear current $\mathbf{j}_{2\omega}$ is perpendicular to the external field $\mathbf{H}$ regardless of which of the components of (7) make up this field. We demonstrate the foregoing using the nonlinearity quadratic in the electric field as the example. In the presence of the field $\mathbf{H}$, the only remaining symmetry operations of the point group $3m$ that describes Bi are those that leave the direction of the external field $\mathbf{H}$ unchanged. At $\mathbf{H} \| C_2 \| z$ this means that the operation of reflection in the xy plane is preserved. In the case corresponding to the upper plot of Fig. 2 we have

$$j_z^{(2\omega)} = \sigma_{zxx}(H) E_x^{(\omega)} E_x^{(\omega)} + \sigma_{zxy}(H) E_x^{(\omega)} E_y^{(\omega)}$$
$$+ \sigma_{zyy}(H) E_y^{(\omega)} E_y^{(\omega)}. \qquad (23)$$

The dependence of the tensor σ_{ijk} on the wave vector $\mathbf{k}$ is immaterial, since $\mathbf{k} \| y$ and the operation of reflection in the xy plane does not affect it. Carrying out the transformation $z \to -z$ we find, for example, that the component $\sigma_{zxx}(H)$ should reverse sign. At the same time, since this transformation is a symmetry operation, and the field $\mathbf{H}$ does not reverse sign (axial vector), we get $\sigma_{zxx}(H) = -\sigma_{zxx}(H) = 0$. Similar reasoning shows readily that in (23) we have $\sigma_{zxy} = \sigma_{zyy} = 0$ and $j_z^{(2\omega)} = 0$.

Since $\mathbf{j}_{2\omega} \perp \mathbf{H}$, the radiation should vanish at $\mathbf{E}_\omega \| z$, as is in fact observed in experiment. The nonlinear current (7) is then different from zero, but is governed only by the alternating magnetic field ($E_y = 0$). A slight tilt of the field $\mathbf{H}$ away from the C_2 axis, by an angle ψ, produces a component of the current $\mathbf{j}_{2\omega}$ along the z axis and a component $E_y \sim \psi$. In this case, according to (5), $P_{2\omega} \neq 0$ but the contribution made to $P_{2\omega}$ by the alternating magnetic field is proportional to ψ^2, and that from the electric field to ψ^4. The nonlinearity connected with the normal electric field E_y can therefore be neglected and the function $P_{2\omega}(H)$ on the lower curve of Fig. 2 can be regarded as the result of only magnetic nonlinearity. When the field $\mathbf{H}$ is tilted away from the C_2 axis by another $0.5°$, the signal $P_{2\omega}$ increases by approximately 6 dB, i.e., by 4 times, thus attesting to the validity of the foregoing statement.

In Figs. 3 and 5 we have $\mathbf{E}_\omega \| \mathbf{E}_{2\omega} \| z$. In this case $E_y \neq 0$ at $\mathbf{H} \| C_1$, but is negligibly small, since it is expressed in terms

of the small component σ_{zy} of the conductivity tensor. At an insignificant deflection of $\mathbf{H}$ away from the C_1 axis the resonance curves have therefore a structure similar to the lower plot of Fig. 2 and can be described within the framework of the model considered.

We discuss now the experiments carried out with an external electric field perpendicular to the surface of the metal. In an isotropic medium, this field falls off towards the interior of the metal faster than the tangential one, although near the surface it is $c/\omega\sigma$ times larger than the transverse electric field (it is advisable to compare the fields at those points of the sample where the magnetic field, and with it the transverse electric, are not small). In an anisotropic medium the external normal electric field penetrates not to the screening depth, but to the skin-layer depth. The reason is that the longitudinal field excites a transverse one, and with it also magnetic fields. Such a field distribution leads to a nonlinear cyclotron resonance in exactly the same manner as in the transverse excitation considered in the preceding section. The relation between the electric and magnetic nonlinearities is determined by the amplitudes of the alternating fields and consequently, when the radius of the diaphragm is changed, the form of the resonance lines in not preserved (Fig. 6). Note the similarity of the lower curve of Fig. 6, when practically the entire sample is uncovered, and the upper curve of Fig. 2. At the lowest amplitude of the alternating magnetic field on the sample, when $R = 1.5$ mm, the integer resonances take the form of distinct maxima. The half-integer resonances $n = 3/2$ and $5/2$ are also maxima, albeit displaced somewhat from the exact position (2) toward weaker magnetic fields. A similar result is observed if the maximum magnetic field is removed from the sample and the electric field perpendicular to the surface is decreased.

The authors thank V. F. Gantmakher and V. S. Édel'man for helpful discussions.

[1] V. T. Dologopolov, Usp. Fiz. Nauk 130, 241 (1980) [Sov. Phys. Usp. 23, 134 (1980)].

[2] A. P. Kopasov, Zh. Eksp. Teor. Fiz. 72, 191 (1977) [Sov. Phys. JETP 45, 100 (1977)].

[3] A. P. Kopasov, ibid. 78, 1408 (1980) [51, 709 (1980)].

[4] A. P. Kopasov, Fiz. Tverd. Tela (Leningrad) 24, 3621 (1982) [Sov. Phys. Solid State 24, 2063 (1982)].

[5] V. F. Gantmakher, G. I. Leviev, and M. R. Trunin, Zh. Eksp. Teor. Fiz. 82, 1697 (1982) [Sov. Phys. JETP 55, 931 (1982)].

[6] M. R. Trunin, Fiz. Tverd. Tela (Leningrad) 27, 2147 (1985) [Sov. Phys. Solid State 27, 1285 (1985)].

[7] V. S. Edel'man, Zh. Eksp. Teor. Fiz. 83, 3217 (1982) [Sov. Phys. JETP 56, 1343 (1982)].

[8] V. S. Édel'man, Usp. Fiz. Nauk 123, 257 (1977) [Sov. Phys. Usp. 20, 819 (1977)].

[9] J. W. McClure and K. H. Choi, Sol. State Comm. 21, 1015 (1977).

[10] G. E. Sith, Phys. Rev. 115, 1561 (1959).

[11] M. R. Trunin, Zh. Eksp. Teor. Fiz. 88, 1834 (1985) [Sov. Phys. JETP 62, 1087 (1985)].

Translated by J. G. Adashko